Thu Dau Mot University Journal of Science
ISSN 2615 - 9635
journal homepage: ejs.tdmu.edu.vn

Applying first principles to study the structural, electronic, and magnetic properties of Pr adsorbed ASiNRs

by ***Thanh Tung Nguyen, Hoang Van Ngoc, Huynh Thi Phuong Thuy, Duy Khanh Nguyen, Vo Van On*** *(Thu Dau Mot University)*

Article Info*: Received Sep.29th, 2021, Accepted Nov. 25th,2021, Available online Dec. 15th,2021*
Corresponding author: onvv@tdmu.edu.vn
https://doi.org/10.37550/tdmu.EJS/2021.04.257

ABSTRACT

Applying first-principles calculations, the investigation of the geometrical and electronic properties of Pr adsorption armchair silicene nanoribbons structure has been established. The results show that the bandgap doped Pr has been changed, which is the case for chemical adsorption on the surface of ASiNRs; this material became metallic with the peak of valance band contact fermi level. Moreover, the survey to find the optimal height 1.82 Å of Pr and 2.24 Å bond length Si-Si, and Si-Si-Si bond angle $108^0 05'$, energy adsorption is -7.65 eV, buckling is 0.43 Å with structure stability close to the pristine case, has brought good results for actively creating newly applied materials for the spintronic and optoelectronics field in the future.

Keywords: *adsorption chemical, metal materials, Pr adsorption*

1. Introduction

Breakthroughs in semiconductor materials and device design frequently accompany the development of electronic and optoelectronic devices. New optoelectronics have good applications, high sensitivity, such as next-generation sensors, field-effect transistors, and many others, in addition to the design needs of electronic devices. Understanding, investigating, and manufacturing novel materials to meet the demands of technological advancement in this field necessitates the involvement of researchers who are pioneers in the field of simulation. Many investigations with monolayer graphene have been Prcoducted for one-dimensional materials (Xinming Li et al., 2020; Cheng, & Goda, 2020; Kai Wu Luo et al., 2016), and germanene findings have been obtained (Acun et al., 2017).

Discuss the effects of boron doping.

The adatom varied geometric shapes, the Si and C dominated energy bands, the spatial charge densities, fluctuations in the spatial charge densities, and the atom and orbital projected density of states (DOSs) were all investigated in the Si adsorbed and replaced monolayer graphene systems (Duy Khanh Nguyen et al., 2020). With three gases, the electrical and transport properties of armchair silicene nanoribbons (ASiNRs) are investigated for use as extremely selective and sensitive gas molecule sensors. By introducing a flaw into ASiNRs, the minimal band gap may be adjusted. The adsorption of NH3 causes the bandgap to open, whereas the adsorption of NO2 causes the bandgap to close.

Density functional theory (DFT) and a variety of Non-Equilibrium Green's function (NEGF) formalisms were used to examine the electrical and optical characteristics of siliphene (carbon-substituted silicene). When the ratio of C to Si is 1:1, carbon-substituted silicene exhibits semiconductor behavior with a bandgap of 2.01 eV (Mostafa Khosravi et al., 2020). Using the DFT approach and the local spin-density approximation, examine the structural and electrical properties of zigzag silicene nanoribbons (ZSiNRs) with edge-chemistry changed by H, F, OH, and O. Three types of spin-polarized configurations are considered: configurations with the same sp^2 hybridizations, configurations with different sp^2 hybridizations, and configurations with different sp^2 hybridizations. The modification of the zigzag edges of silicene nanoribbons is a key issue to apply the silicene into the field-effect transistors (FETs) and gives more necessity to better understand the experimental findings (Yin Yao et al., 2016).

In the case of Pr, the results from experimental studies by different authors show that Pr can combine with Si to form compounds with different valences such as PrSi, Pr_3Si_2, Pr_5Si_3, Pr_5Si_4, Pr_3Si , $PrSi_2$. All these compounds are metallic and magnetic with a bandgap Eg = 0, densities from 5 to 6.5 g/cc. However, no simulation study results have been published from doping Pr with Silicene with armchairs or zigzag forms (Guang Tian et al., 2019; Haifang Yang et al., 2003; de la Venta a,n et al., 2013; Yusuke Saito et al., 2013).

2. Computational detail

The DFT approach is used to explore the structural and electrical properties of Pr adsorption silicene nanoribbons. The VASP software suite is used to complete all of the calculations. Under the generalized gradient approximation, the many-body exchange and correlation energies resulting from electron-electron Coulomb interactions are calculated using the Perdew–Burke–Ernzerhof (PBE) functional. Furthermore, the projector-augmented wave (PAW) pseudopotentials characterize the intrinsic electron-ion interactions. The kinetic energy cutoff for the entire set of plane waves is set to 400

eV, which is sufficient for analyzing Bloch wave functions and electronic energy spectra. For geometry optimization and static total energy, electronic structures, 1x1x12 and 1x1x100 k-point meshes within the Monkhorst-Pack sample the Brillouin zone. During ionic relaxations, the greatest Hellman-Feynman force acting on each atom is less than 0.01 eV/Å, and the ground-state energy convergence is 10^{-6} eV between two successive steps.

The adsorption energy is used to determine the stability of Pr adsorption on Pristine.

$$\text{Delta E} = E_{System} - E_{Metal} - E_{Pristine} \quad (1)$$

where E_{Metal}, $E_{Pristine}$ and E_{System} are the total energy of Pr atom metal, Pristine, and Pr adsorbed on Pristine (Feng et al., 2012).

3. Results and discussion

3.1 Structural properties

Building a survey model based on a monolayer ASiNRs model with N of 6 is described (see Figure 1). The model comprises a fundamental structure of 12 C atoms and 4 H atoms, with Pr as the metal of study. We investigate the electrical properties and geometrical structure of the Pr doped system and pristine ASiNRs through 3 basic steps as follows:

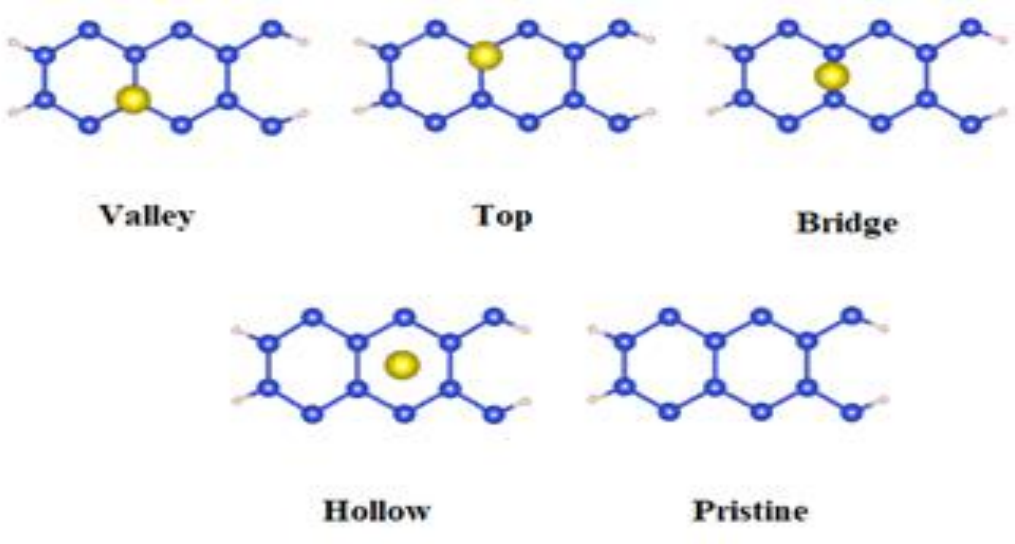

Figure 1. *Valley, Top, Bridge, Hollow positions, and pristine ASiNRs*

In the first step, we investigate the optimal case between 4 basic positions, top, valley, bridge, and hollow for the case of bond length is 2.5 Å and 8.4 Å height. The obtained results show that all 4 sites have similar adsorption factors, but the hollow site has the largest chemisorption energy of -3.83eV with the smallest buckling of 0.40 Å and Pr is stable at average high compared to other cases is 7.28 Å, h is the distance from Pr to the plane containing 3 Si atoms at the top positions (see Table 1). The structure of the

hollow case system is stable, the average bond angle is $117^0$26', the honeycomb configuration is slightly expanded compared to the original pristine angle, which is $108^0$05' and Magne is -0.64 μ_B.

TABLE 1. The calculation results correspond to the Top, Valley, Bridge, and Hollow

	Valley	**Top**	**Bridge**	**Hollow**	**Pristine**
$E_{Pristine}$ (eV)	-69.5636	-69.5636	-69.5636	-69.5636	-69.5636
E_{Metal} (eV)	-0.45	-1.55	-1.84	1.74	X
E_{System} (eV)	-67.4977	-72.59	-72.56	-71.65	X
Delta E (eV)	2.52	-1.48	-1.15	**-3.83**	X
Buckl (Å)	0.43	0.43	0.42	0.40	0.44
h (Å)	7.40	6.14	7.64	7.28	X
Angle (deg)	$116^0$46'	$116^0$43'	$116^0$52'	$117^0$26'	$108^0$05'
Mag (μ_B)	4.08	2.80	2.80	-0.64	0.00
Bandgap (eV)	0	0	0	0	0.5423
Structure states	M	H	M	H	H

In the second step, we consider the hollow position but change the d_0 bond length from 2.20 Å to 2.32 Å for the same height of 8.4 Å.

TABLE 2. Calculation results corresponding to different bond lengths d_o

d_o	**Delta E (eV)**	**Mag (μ_B)**	**Buckl (Å)**	**h (Å)**	**Angle (deg)**	**Pristine (deg)**	**States structure**
2.20	-1.12	2.79	0.61	5.36	$114^0$28	$108^0$05	L
2.21	0.07	1.35	0.70	2.26	$112^0$27	$108^0$05	L
2.22	3.52	-1.24	0.61	5.36	$114^0$28	$108^0$05	L
2.23	-0.26	-3.56	0.56	5.88	$111^0$35	$108^0$05	L
2.24	-3.23	-2.80	0.80	6.38	$108^0$05	$108^0$05	H
2.25	-0.40	-2.79	0.81	6.41	$108^0$05	$108^0$05	H
2.26	-1.66	2.80	0.54	6.65	$114^0$53	$108^0$05	H
2.27	-0.33	2.80	0.81	6.47	$108^0$05	$108^0$05	H
2.28	0.72	1.15	0.63	2.67	$113^0$44	$108^0$05	M
2.29	-7.64	-2.50	0.52	6.75	$115^0$13	$108^0$05	M
2.30	-2.45	2.63	1.87	1.95	$109^0$43	$108^0$05	L
2.31	-0.91	2.79	0.77	6.51	$109^0$34	$108^0$05	M
2.32	6.67	3.00	0.40	4.82	$117^0$34	$108^0$05	M

With the formation of the synthetic structure after chemical adsorption between Pr and pristine, the structural forms are divided into 3 levels, namely H (high), M (middle), and L (low) with stable levels. from high to low as shown in Table 2. Calculation results are obtained, the bond length from 2.24 Å to 2.27 Å is the allowable range for the doped system to have the best stable configuration H level. More precisely corresponds to a bond length of 2.24 Å with a bond energy of -3.32eV, a height of 6.38 Å, and an angle of deviation between the three Si atoms of $108^0$05 which resembles the corresponding pristine structure (see Table 2).

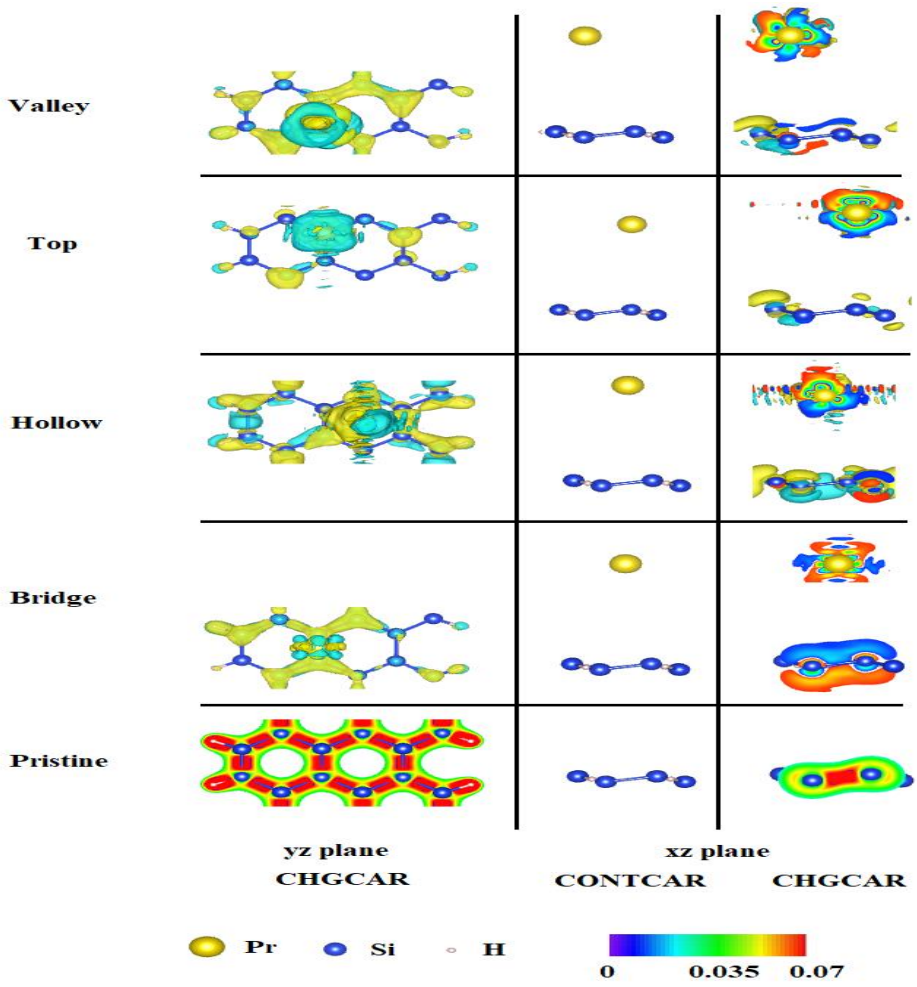

Figure 2. *Results of drawing CONTCAR, CHGCAR files with different positions*

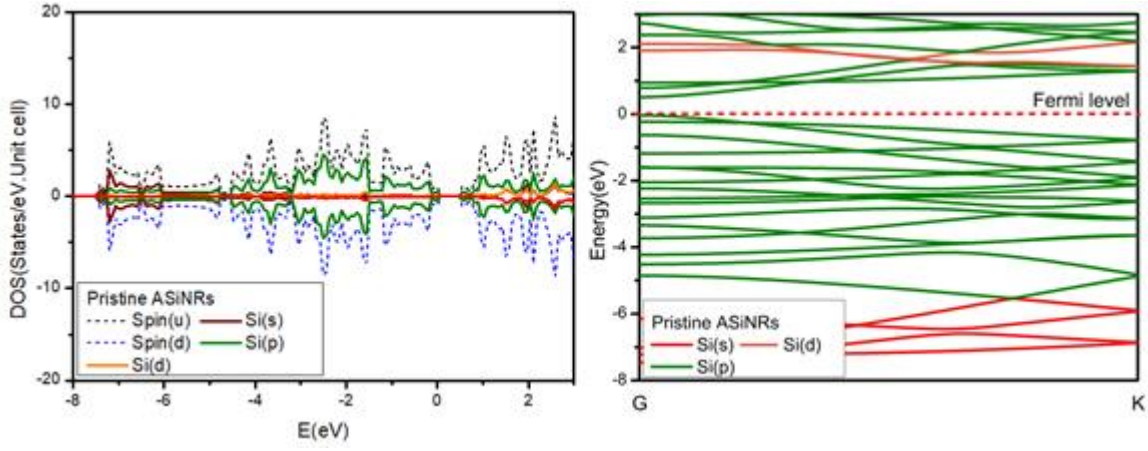

Figure 3. *Band and DOS structure of pristine AsiNRs*

In the third step, we respectively investigate the bond length 2.24 Å at different defined initial heights from 5.2 Å to 8.6 Å with the POSCAR file. Calculation results show that the altitude corresponding to chemical adsorption with a stable structure of 1.78 Å has an optimal energy level of -7.65 eV and a corresponding magnetic moment here of -3.2

which is larger than the other positions. neighborhood location (See Table 3). At elevations of 6.1 Å to 6.8 Å (respectively initial height 8.2 Å to 8.6 Å), the structural states are also stable but with energies lower than -4.75eV to -2.07eV, we assume that these are physically absorbed Pr atomic sites.

3.2. Electronic propeties

In this section, the results of calculating the region structure and density of states (DOS) of pristine and Pr/pristine are presented and analyzed with Spin_up (blue, short dash), Spin_down histograms. (black, short dash), Si(s)-wine, Si(p)-olive , Pr(s)-pink, Pr(p)-cyan, Pr(d)-red, and Pr (f)-blue.

The electronic and DOS band structure of pristine before Pr adsorption is presented in Figure 3 to compare the similarities and differences in adsorption. Using DFT to calculate the results, the region structure after Pr adsorption has the same characteristics in some orbital layers such as Si(s) and Si(p), in both cases shown in Figure 3 plotted in the Brillouin (GK) region with energies from -8 eV to 3 eV and a k point index from 0 to 0.08.

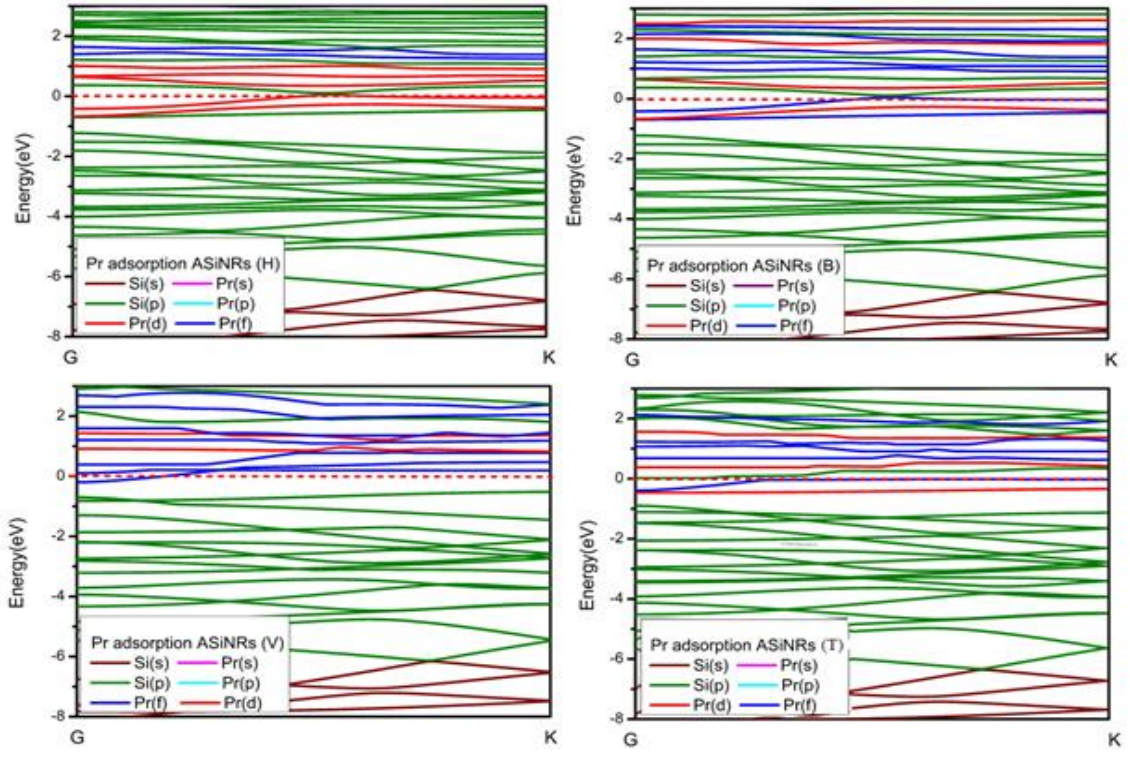

Figure 4. *Band structures of Hollow (H), Bridge (B), Valley (V), and Top (T)*

The relationship between pristine buckling δ and bond length d_{Si-Si} is inversely proportional to each other and is shown through Figure 3.

The important results clearly show that the valence band maxima (VBM) exposed to Fermi level energies (the Fermi level is determined at 0) means that the post-doping material is metallic, whereas pristine pre-doping is a semiconductor with the bandgap

energy is 0.5423 eV. When considering the energy levels in the band structure, it is shown that the s, p, and d orbitals electrons of Si are all involved in the change in electron density in the junction between the Si atoms and the adsorbed Pr atoms. The Pr(d) orbital in the vicinity of the fermium level and in the range -0.57 eV to 0.82 eV, and Pr(f) orbital in the range 0.2 eV to 1.44 eV which are the main factor causing sp and sp^2 hybridization when electrons from Pr exert bond-breaking forces.

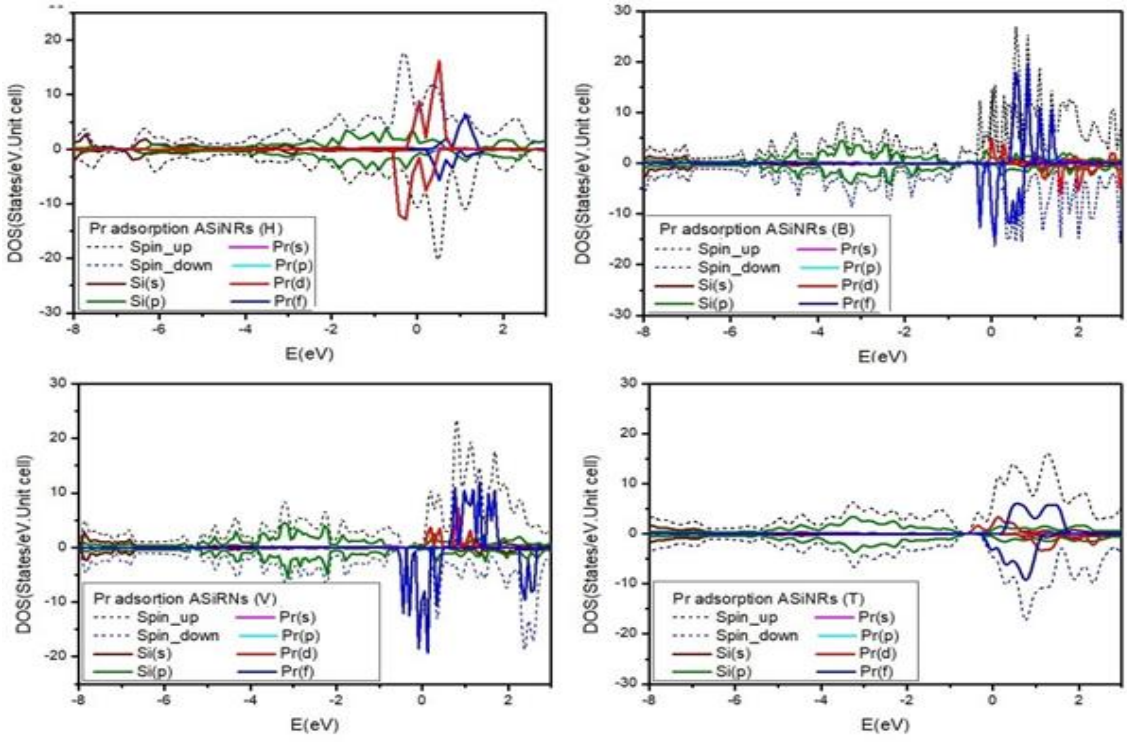

Figure 5. *DOS structures of Hollow (H), Bridge (B), Valley (V), and Top (T)*

The occurrence of peaks at 0.51 eV, 0.05 eV, -0.26 eV, and 0.2 eV in DOS demonstrates that there is strong participation in the charge exchange in the orbitals when adsorbing Pr (d). Besides, the peaks are very strong and wide, corresponding to Pr(f) is 1.13eV, 0.12eV, and 0.82 eV while in the pristine case these peaks are absent (see Figure 5).

In the case of DOS structures results shown in Figure 5 are for other locations such as valley, top, and bridge. We do not analyze it in depth here, because a glance is similar to the case at the hollow position, but shows that the charge displacement in the regions is relatively weak compared to the hollow case that we presented in the previous section. above, showing that hollow is the most optimal position chosen.

The magnetic properties of silicene adsorbed with Pr transition metal (TM) atom have been investigated by using spin-polarized DFT calculations Pr adatoms are considered to prefer to bind to the hexagon hollow site of silicene. A strong covalent bonding character between the Pr adatom and Silicene layer is found in most Pr/silicene adsorption systems. Through adsorption, show the Silicene's electronic and magnetic

properties. The adatoms all generate nearly integer magnetic moments. The effects of the on-site Coulomb interaction as well as the magnetic interaction between Pr adatoms on the stability of the half-metallic Pr/silicene systems are also considered, and the results show that the half-metallic state for the Pr/silicene is strong. The ferromagnetic Pr/silicene system should have potential applications in the fields of one-dimensional spintronics devices. The analysis of the DOS indicates the ferromagnetic property of the obtained Pr/silicene system mainly resulted from the spin-split of the Pr (3d) and Pr(4f) states (Feng et al., 2012; Mu Lan et al., 2013).

TABLE 3. Result calculation of different hight Pr

ho (Å)	**Delta E (**eV**)**	**Mag (**μB**)**	**h** (Å)	**Buckl** (Å)	**States structure**
8.6	-2.07	2.80	6.77	0.55	H
8.4	-2.98	-2.79	6.51	0.56	H
8.2	-4.75	2.79	6.09	0.58	H
8.0	-1.38	2.79	5.71	0.56	M
7.8	-1.51	2.77	5.29	0.57	M
7.6	-1.20	2.79	4.72	0.53	M
7.4	-4.20	3.01	1.69	0.17	L
7.2	-3.61	3.01	1.87	0.52	L
7.0	-7.65	-3.02	1.78	0.43	H
6.8	-4.32	-3.02	1.80	0.63	M
6.6	-4.16	3.00	1.82	0.32	M
6.4	-5.49	2.98	1.80	0.45	M
6.2	-5.69	2.95	1.89	0.38	H
6.0	-5.38	2.91	1.83	0.47	M
5.8	-4.28	2.90	1.80	0.31	H
5.6	-4.76	2.96	1.85	0.45	H
5.4	-4.47	2.84	1.84	0.49	H
5.2	-5.04	3.00	0.10	0.80	H

The multi-orbital hybridizations in chemical bonds, which are responsible for the adatom-diversified geometric structures, electronic band structures, and density of states, can be delicately identified from the spatial charge densities and their variations under the various modifications. The latter is obtained from the difference between the Pr-adsorption and pristine cases (Chen et al., 2012).

A review of the data on the number of electrons of the orbitals in the respective Pr/ASiNRs chemisorption systems for the hollow site shows that pristine does not exist f orbital (The electron configuration of Si is $1s^2\ 2s^2\ 2p^6\ 3s^2,\ 3p^2$). When Pr/ASiNRs chemisorption, electrons are involved in the s, p, d, f orbitals of the Pr atom (The electron configuration of Pr is [Kr] $5s^2\ 4d^{10}\ 5p^6\ 4f^3,\ 6s^2$) leads to electron exchange, and hybridization also occurs here. This is shown in the band and DOS structures in the presence of adsorption and disadsorption. However, based on the calculation results and the band structure and DOS

drawings, it shows that the participation is mainly electrons in the d and f orbitals of the Pr atom, and very little for s and p (see Figures 3, 4). The electron configurations for Pr adatoms adsorbed pristine at hollow with result pristine ($3d^{1.40}$, $3p^{17.79}$, $3s^{13.60}$, $tot^{32.79}$), Pr is ($4f^{3.31}$, $4d^{0.03}$, $5p^{5.36}$, $6s^{1.99}$, $tot^{10.68}$), and Pr/ASiNRs ($f^{0.21}$, $d^{1.96}$, $p^{24.26}$, $s^{16.03}$, $tot^{42.47}$).

Based on the calculation results, the electron charge density in the orbitals before and after Pr/ASiNRs adsorption shows that, in the d orbital, the electron charge has shifted from the 3d orbital (Si) to 1.40 e/ $Å^3$ to combine electrically element in orbital 4d (Pr) 0.03 e/ $Å^3$ forms orbital d of system 1.96 e/ $Å^3$ with enhancement from other orbitals. Besides, orbital 4f (Pr) 3.31 e/ $Å^3$ electron charge decreased from 0.21 e/$Å^3$ upon adsorption, showing that part of the charge has transferred to the d orbital; for the p orbital, the number of electron charges in the 5p (Pr) orbital 5.36 e/ $Å^3$ combined with 3p (Si) 17.79 e/ $Å^3$ forms a concentration of 24.26 e/ $Å^3$ when adsorbing Pr/ASiNRs as accept/give electrons are rare. With the s orbital being a combination of 6s (Pr) orbital 13.60 e/ $Å^3$ combined with 1.99 e/ $Å^3$ from 3s (Si) pristine for a total of 16.03 e/ $Å^3$ in Pr/ASiNRs with few extra electrons. In summary, during chemisorption, there is a shift of electron charge from the 4f orbital (Pr) to the 3d orbital (Si) and a small part to 5p(Pr) of the Pr/ASiNRs system (see Figure 4). The results also correspond to the studies on the adsorption of metals on SiNRs or gemanene, graphene that the authors presented (Chen et al., 2013; Nzar Rauf Abdullahab et al., 2021; Pang et al., 2015; Wenhao Liu et al., 2017; Gurleen Kaur Walia et al., 2018; Daniel Bahamon et al., 2021; Kent Gang et al., 2013; Yongxiu Sun et al., 2019; Vogt et al., 2012; Paola et al., 2011).

4. Conclusion

In this project, we apply density function theory to calculate and investigate the electronic, magnetic and geometrical properties of the chemisorption between Pr and ASiNRs.The first step considers the optimal case for the top, valley, bridge and hollow sites the same bond length and distance from Pr to pristine. The results show that the hollow site is the most ideal in terms of adsorption energy as well as structural stability. In the second step, we investigate the case of changing the bond length of Si-Si in pristine for the adsorption of Pr/ASiNRs. In the last step, we investigated the change in Pr elevation related to the chemical adsorption capacity of Pr on the pristine background. As a result, we found optimal cases where the resulting compound is a magnetic metal which is a good candidate for the development of new generation electronics or spintronics.

Acknowledgments

This research is funded by Thu Dau Mot University, Binh Duong Province, Vietnam, under grant number DA.21.1-004, and this research used resources of the high-performance computer cluster (HPCC) at Thu Dau Mot University, Binh Duong Province, Vietnam.

References

A Acun, L Zhang, P Bampoulis, M Farmanbar, A van Houselt, A N Rudenko, M Lingenfelder, G Brocks, B Poelsema, M I Katsnelson (2017). Germanene: the germanium analogue of graphene. *Journal of Physics: Condensed Matter*, *27*(44), 443002.https://iopscience.iop.org/article/10.1088/0953-8984/27/44/443002

Chen L, Li H, Feng B, Ding Z, Qiu J, Cheng P, Wu K and Meng S. (2013). Spontaneous Symmetry Breaking and Dynamic Phase Transition in Monolayer Silicene. *Phys. Rev. Lett*, 110, 85504. https://doi.org/10.1103/PhysRevLett.110.085504

Chen L, Liu C-C, Feng B, He X, Cheng P, Ding Z, Meng S, Yao Y and Wu K.(2012). Evidence for Dirac Fermions in a Honeycomb Lattice Based on Silicon. *Phys. Rev. Lett*, 109, 56804. https://doi.org/10.1103/PhysRevLett.109.056804

Cheng, Z., and Goda, K. (2020). Design of waveguide-integrated graphene devices for photonic gas sensing. *Nanotechnology*, 27 (50), 505206. https://10.1088/0957-4484/27/50/505206

Daniel Bahamon, Malathe Khalil, Abderrezak Belabbes, Yasser Alwahedi, Lourdes F. Vega, Kyriaki Polychronopoulou.(2021). A DFT study of the adsorption energy and electronic interactions of the SO_2 molecule on a P hydrotreating catalyst. *ARC Advances*, 11(5), 2947-2957. https://doi.org/10.1039/C9RA10634K

Duy Khanh Nguyen, Ngoc Thanh Thuy Tran, Yu-Huang Chiu, Godfrey Gumbs, Ming-fa Lin (2020). Rich essential properties of Si-doped graphen, *Scientific reports, Open Access*, 10, 12051. https://doi.org/10.1038/s41598-020-68765-x

Duy Khanh Nguyen, Ngoc Thanh Thuy Tran, Yu-Huang Chiu, Godfrey Gumbs, Ming-fa Lin (2020). Rich essential properties of Si-doped graphene. *Scientific Reporst*, 10, 12051https://doi.org/10.1038/s41598-020-68765-x

Feng B, Ding Z, Meng S, Yao Y, He X, Cheng P, Chen L and Wu K. (2012). Evidence of Silicene in Honeycomb Structures of SiliPrn on Ag(111). *Nano Lett***,** 12, 3507–11.https://doi.org/10.1021/nl301047g

Guang Tian, Honglin Du, Wenyun Yang, Changsheng Wang, Jingzhi Han, Shunquan Liua, JinboYang (2019). Structural and magnetic properties of Pr_5Si_3-xGe_x compounds, *Journal of Alloys and Compounds*, *788*(5), 468-475. https://doi.org/10.1016/j.jallcom.2019.02.172

Gurleen Kaur Walia, Deep Kamal Kaur Randhawa (2018). First-principles investigation on defect-induced silicene nanoribbons — A superior media for sensing NH_3, NO_2 and NO gas molecules. *Surface Science*, 670, 33-43. https://doi.org/10.1016/j.susc.2017.12.013

Gurleen Kaur Walia, Deep Kamal Kaur Randhawa. (2018). Gas-sensing properties of armchair silicene nanoribbons towards carbon-based gases with single-molecule resolution. *Structural Chemistry*, 29, 1893-1902. https://doi.org/10.1007/s11224-018-1170-9

Haifang Yang, G. H. Rao, Guangyao Liu, J. K. Liang (2003). Crystal structure and magnetic properties of Pr_5Si_4-xGe_x compounds, *Journal of Magnetism and Magnetic Materials*, *263*(1-2), 146-153. http://dx.doi.org/10.1016/S0304-8853(02)01548-2

J. de la Venta a,n , Ali C. Basaran a,b , T. Grant c , J.M. Gallardo-Amores d , J.G. Ramirez a, M.A. Alario-Franco d , Z. Fisk c , Ivan K. Schuller (2013). Magnetism and the absence of superconductivity in the praseodymium–silicon system doped with carbon and boron. *Journal of Magnetism and Magnetic Materials*, 340, 27-31.https://doi.org/10.1016/j.jmmm.2013.03.018

Kai Wu Luo, Liang Xu, Ling Ling Wang, Quan Li, Zhiyong Wang (2016). Ferromconetism in zigzag GaN nanoribbons with tunable half-metallic gap. *Computational Materials Science*. https://doi.org/10.1016/j.commatsci.2016.02.012

Kent Gang, Siva Gangavarapu, Matthew Deng, Max Mcgee, Ron Hurlbut, Michael Lee Dao Kang, Sean NG Peng Nam, Harman Johll, Tok Eng Soon (2013). Fe, Pr and Ni Adatoms Adsorbed On Silicene: A DFT Study, *Singapore International Science Challenge Proceedings*. 80-93. https://digitalPrmmons.imsa.edu/student_pr/9/

Mostafa Khosravi, Gholamali Moafpourian, Hojat Allah Badehian (2020). Optical spectra of carbon-substituted silicene: A first principle study. *Optics*, 218, 165247.https://doi.org/10.1016/j.ijleo.2020.165247

Mu Lan, Gang Xiang, Chenhui Zhang, *and* Xi Zhang (2013). Vacancy dependent structural, electronic, and magnetic properties of zigzag silicene nanoribbons: Ag. *Journal of Applied Physics*, 114, 163711. https://doi.org/10.1063/1.4828482

Nzar Rauf Abdullahab, Mohammad T.Kareemc, Hunar Omar Rashida, Andrei Manolescud,Vidar Gudmundssone.(2021). Spin-polarised DFT modeling of electronic, magmnetic, thermal and optical properties of silicene doped with transition metals. *Physica E: Low-dimensional and Nanostructures*, 129, 114644. https://doi.org/10.1016/j.physe.2021.114644

Paola De Padova,Claudio Quaresima, Bruno Olivieri, Paolo Perfetti, Guy Le Lay (2011). sp2-like hybridization of silicon valence orbitals in silicene nanoribbons. *Applied physics letters*, 98, 081909. https://doi.org/10.1063/1.3557073

Q. Pang, Long Li, C. Zhang, Xiumei Wei, Y. Song (2015). Structural, electronic and magnetic properties of 3d transition metal atom adsorbed germanene: A first-principles study. *Materials Chemistry and Physics*, 160, 96-104. https://doi.org/10.1016/j.matchemphys.2015.04.011

Vogt P, De Padova P, Quaresima C, Avila J, Frantzeskakis E, Asensio M C, Resta A, Ealet B and Le Lay G.(2012). Silicene: compelling Experimental Evidence for Graphenelike Two- Dimensional Silicon. *Phys. Rev. Lett*, 108, 155501.https://doi.org/10.1103/PhysRevLett.108.155501

Wenhao Liu, Jiming Zheng, Puju Zhao, Shuguang Cheng, Chongfeng Guo. (2017). Magnetic properties of silicene nanoribbons: A DFT study. *AIP Advances*, 7, 065004.https://doi.org/10.1063/1.4985139

Xi Chen, Jun Ni (2013). Predicted ferrom Prnetism in hole doped armchair nanoribbons: A first principles study. *Chemical Physics Letters*, *555*(3), 173-177.

Xinming Li, Xu Zhang, Hyesung Park, Antonio Di Bartolomeo (2020). Editorial: Electronics and Optoelectronics of Graphene and Related 2D Materials. *Frontiers in Materials*. https://doi.org/10.3389/fmats.2020.00235

Yin Yao, Anping Liu, Jianhui Bai, Xuanmei Zhang, Rui Wang (2016). Electronic Structures of Silicene Nanoribbons: Two-Edge-Chemistry Modification and First-Principles Study. *Nanoscale Res Lett*, 11, 371. https://dx.doi.org/10.1186%2Fs11671-016-1584-5

Yongxiu Sun, Aijian Huang, Zhiguo Wang (2019). Transition metal atom (Ti, V, Mn, Fe, and Co) anchored silicene for hydrogen evolution reaction. *RSC Adv.*, 9, 26321-26326https://doi.org/10.1039/C9RA04602J

Yusuke Saito, Norio Nakata, Akihiko Ishii (2013). Copolymerization of Ethylene with iPr_3Si-Protected 5-Hexen-1-ol with an [OSSO]-Type Bis(phenolato) Dichloro Zirconium(IV) Complex. *Bulletin of the Chemical Society of Japan*, *89*(6), 666-670. https://doi.org/10.1246/bcsj.20160043